

## **Synthesis and Characterization of Fe<sub>3</sub>O<sub>4</sub> stabilized ZrO<sub>2</sub> Nanoparticles**

\* Mahwish Bashir<sup>1)</sup>, Saira Riaz<sup>2)</sup>, M Saeed Akhtar<sup>3)</sup> and Shahzad Naseem<sup>4)</sup>  
Centre of Excellence in Solid State Physics, University of the Punjab, Lahore, Pakistan  
[\\*shahzad\\_naseem@yahoo.com](mailto:shahzad_naseem@yahoo.com)

### **ABSTRACT**

The availability of zirconium dioxide (zirconia) ceramics in dentistry has expanded the range of designs and applications for all-ceramic restorations and increased its popularity. Nanoparticles (NPs) have attracted considerable attention owing to their unique properties and ease of production from variety of materials. Zirconia with enhanced properties can be achieved by doping with biocompatible material. The present study devised sol gel method for preparation of Fe<sub>3</sub>O<sub>4</sub> doped ZrO<sub>2</sub> nanoparticles (NPs). Zirconia sol is doped with pre-synthesized Fe<sub>3</sub>O<sub>4</sub> NPs. Structural characterizations have shown a mixture of monoclinic and tetragonal zirconia. An increase in crystallite size has observed with dopant concentration. Lattice contraction was observed for the Fe<sub>3</sub>O<sub>4</sub>-doped zirconia samples. This lattice contraction results in volumetric change which leads to formation of tetragonal phase. Relative higher density (~6g/cm<sup>3</sup>) has been observed which is requisite for implantations and coatings. Magnetic properties reveal the mix paramagnetic and ferromagnetic behavior with low value of coercivity and magnetization.

### **1. INTRODUCTION**

Ceramic bio-materials are frequently used in orthopedics and dental applications (Nascimento et al. 2007). For example, ceramics are used in numerous applications especially in biomedical field because of their low friction surface and low debris products (Nilsson et al. 2010). Moreover, ceramic materials also demonstrated high biocompatibility properties (Wei and Ma 2004). Among ceramic zirconium oxide (ZrO<sub>2</sub>) is considered as a dynamic ceramic material because of its excellent chemical, structural and mechanical properties used in myriad applications for example catalysts, oxygen sensors, fuel cells, teeth coatings and implantations etc. (Muller et al. 2004). Recently, nanocrystalline materials, especially zirconia (ZrO<sub>2</sub>) nanoparticles (NPs), have gained a lot of interest due to their exceptional physical and structural properties, which are significantly different from their microcrystalline complements (Kazemi 2011).

Pure zirconia exists in amorphous and three crystalline phases: monoclinic, tetragonal and cubic structures, which are thermo-dynamically stable at different temperatures (Li et al. 2013). Monoclinic phase (m-phase) is stable at temperature below 1172°C, tetragonal phase (t-phase) stable at temperature below 1170°C, and cubic phase (c-phase), stable above 2347 °C (Kohorst et al. 2012, Balakrishnan et al.

---

1), 3) Graduate Student

2), 4) Professor

2013). Different crystal structures and phases have numerous applications. C-phase of zirconia is widely used for solid oxide fuel cells (SOFCs), oxygen sensors, electrochemical capacitor and electrode sand ferrules due to its ionic, electrical and optical properties. Among all phases of zirconia tetragonal phase has high value of hardness and compatible for the implants in dentistry and orthopedics (Davar et al. 2013).

But tetragonal zirconia phase is unstable at ambient conditions (Silva et al. 2011). Upon cooling, t-phase transform into monoclinic at room temperature. Up to now different metal oxides such as,  $Y_2O_3$ , CaO,  $CeO_2$  have been used to stabilize zirconia at room temperature and enhance its biological applications era and properties (Fischer and Kersch 2008). This stabilization can be performed by charge imbalance of substitution of atoms of different valences (Beg et al. 2007). However, recent in vitro works demonstrated, in the limit of these experiments, the stability of the yttria doped ceramics to these treatments by various parameters analysis. Moreover, yttria addition in zirconia for stabilization is not suitable for treatment of cancer due to its too short half-life. Consequently the radioactivity of the microspheres may substantially decay even before the cancer treatment (Somiya et al. 2006). In such case iron oxide is an efficient stabilizer and its biocompatibility has already been proven. Doping of iron oxide in zirconia leads to stabilization of tetragonal phase at room temperature (Bashir et al. 2014).

Doped zirconia NPs have been synthesized using different experimental techniques such as co precipitation, ball milling and sol gel etc. Sol gel synthesis is better due to its numerous advantages such as, it has low processing temperature and it can change the material properties by changing the composition of the precursor. It has ability to control size and shape of the particles, low processing temperature and excellent control of microstructures (Riaz et al. 2013).

In this research article we have synthesized  $Fe_3O_4$  doped  $ZrO_2$  nanoparticles at different concentration of  $Fe_3O_4$  and their structural and magnetic properties are investigated.

## **2. EXPERIMENTAL DETAILS**

$ZrOCl_2 \cdot 8H_2O$  (Sigma–Aldrich, 99.99% pure),  $FeCl_3 \cdot 6H_2O$  (Sigma–Aldrich, 99.99% pure),  $FeCl_2 \cdot 4H_2O$  (Sigma–Aldrich, 99.99% pure) and  $NH_3$  (Sigma–Aldrich, 99.99% pure) were used without further purification. Water was deionized (DI) prior to use.

### *2.1 Synthesis of Nanoparticles*

Zirconium oxychloride octahydrate ( $ZrOCl_2 \cdot 8H_2O$ ) was used as a precursor of zirconia, which was mixed in DI water to form 0.1M solution.  $NH_3$  was added into 0.1M solution of zirconium oxychloride to form a milky sol. Shiny and transparent sol was obtained after stirring at a temperature of 50°C. Pre-synthesized NPs  $Fe_3O_4$ , through a modified co-precipitation route (Riaz et al. 2014) was doped in 2-6 wt%. Doped zirconia sol was stirred at 60°C until gel obtained. Gels of doped zirconia were dried at 70-80°C for formation of powders.

### *2.2 Characterizations*

A wide angle X-ray diffractometer (Bruker D8 Advance) was used to study the crystalline structure of the NPs. The Cu K-alpha radiation source was used. K-beta filter was used to eliminate interference peak. Magnetic properties were investigated by using Lakeshore 7407 vibrating sample magnetometer.

### 3. RESULTS AND DISCUSSION

XRD patterns of as-synthesized  $\text{Fe}_3\text{O}_4$  doped zirconia NPs show polycrystalline nature at all concentrations as depicted in Fig. 1. At 2-6wt% concentration of  $\text{Fe}_3\text{O}_4$ , peaks at approximately  $22.0^\circ$ ,  $31.8^\circ$ ,  $39.9^\circ$  and  $46.1^\circ$  correspond to the (011), (111), ( $\bar{2}11$ ) and (-202) planes of monoclinic zirconia (m- $\text{ZrO}_2$ ) [JCPDS 81-1314]. However, peaks correspond to  $59.0^\circ$ ,  $68.8^\circ$ ,  $73.5^\circ$  and  $78.1^\circ$  correspond to the (221), (123) (004) and (330) planes of tetragonal zirconia (t- $\text{ZrO}_2$ ) [JCPDS 17-923], respectively.  $\text{Fe}_3\text{O}_4$  results in partially stabilized zirconia (PSZ) at room temperature. However, as the  $\text{Fe}_3\text{O}_4$  concentration increases up to 6wt%, intensity of tetragonal peak along (211) plane increases and intensity of m (111) reduces. This means  $\text{Fe}_3\text{O}_4$  stimulates the phase transformation from monoclinic to tetragonal. Reduction in monoclinic content in  $\text{Fe}_3\text{O}_4$  doped  $\text{ZrO}_2$  NPs is due to substitution of Fe ions with Zr ions. When a Fe ion replaces Zr ions oxygen vacancies are created and distortion in lattice structure formed (Bashir et al 2014a).

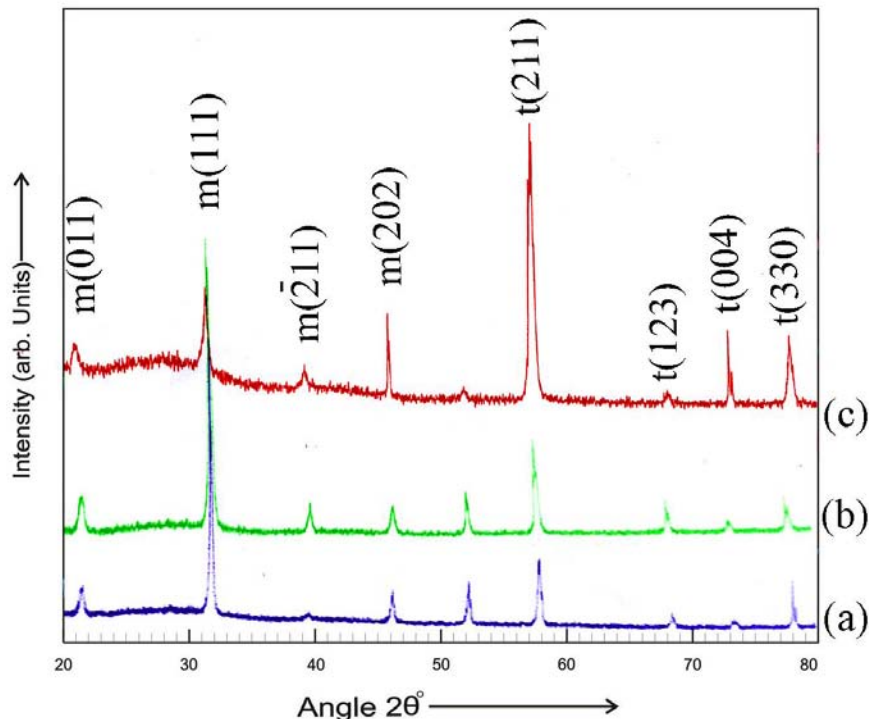


Fig. 1 XRD Patterns of doped zirconia NPs at (a) 2, (b) 4 and (c) 6wt%

Volume fraction of monoclinic phase ( $V_m$ ) was calculated by the following equations, as given in Eqs. 1-2 (Sahu and Rao 2000);

$$X_m = \frac{I_m(111) + I_m(011)}{I_t(211) + I_m(111) + I_m(011)} \quad (1)$$

$$V_m = \frac{(1.311X_m)}{1 + (0.311X_m)} \quad (2)$$

Where,  $I_m$  and  $I_t$  denote to the intensities of monoclinic and tetragonal peaks respectively. Whereas, volume fraction of tetragonal phase was calculated by using Eq. 3;

$$V_t = 1 - V_m \quad (3)$$

Volume fraction of monoclinic phase decreases with the  $Fe_3O_4$  content. The volume fraction ratio of monoclinic and tetragonal  $Fe_3O_4$  nanopowders is calculated by Eq. 2. The results are summarized in Table 1. The fraction of t-phase retained at room temperature may be due to creation of oxygen vacancies attributed by substitution of divalent ( $Fe^{2+}$ ) and trivalent ( $Fe^{3+}$ ) atoms (Bashir et al. 2014b).

Table 1. Variation in tetragonal to monoclinic ratio (t:m) with reaction temperature

$Fe_3O_4$ Concentration (wt%)	t:m
2	23:77
4	26:74
6	56:64

Crystallite size was calculated by using Debye Scherer's formula is given in Eq. 4 (Cullity 1956).

$$D = \frac{0.9\lambda}{\beta \cos\theta} \quad (4)$$

Where D is grain size of the  $Fe_3O_4$  doped  $ZrO_2$  powders,  $\beta$  is the width at half maximum (FWHM) of a Bragg peak,  $\lambda$  is the X-ray wavelength ( $1.5406\text{\AA}$ ) and  $\theta$  is the Bragg angle. Crystallite size of  $Fe_3O_4$  doped zirconia is larger for low doping concentration (2wt%). However, as the  $Fe_3O_4$  content increases [Fig. 2]. A decrease in crystallite size has observed. This decrease in crystallite size is due to substitution of different atomic radius of dopant. Dislocation lines/ $m^2$  was calculated by using formula  $1/D^2$ , where D is crystallite size calculated from Scherer's formula. Very less defects in material lead to strong bonding between atoms which are preferable for biological implants and cure diseases.

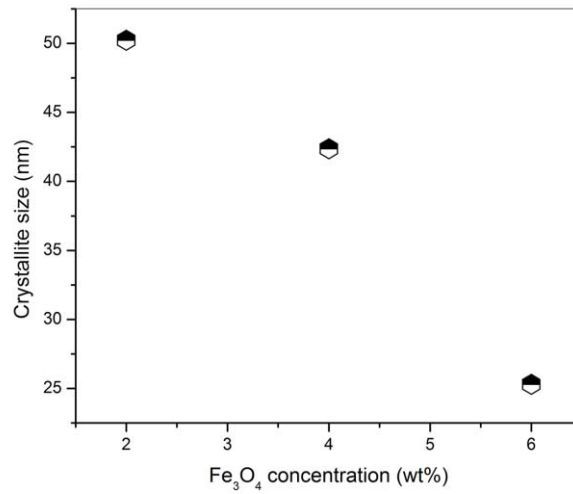


Fig. 2 Crystallite size of doped zirconia NPs as a function of Fe<sub>3</sub>O<sub>4</sub> concentrations

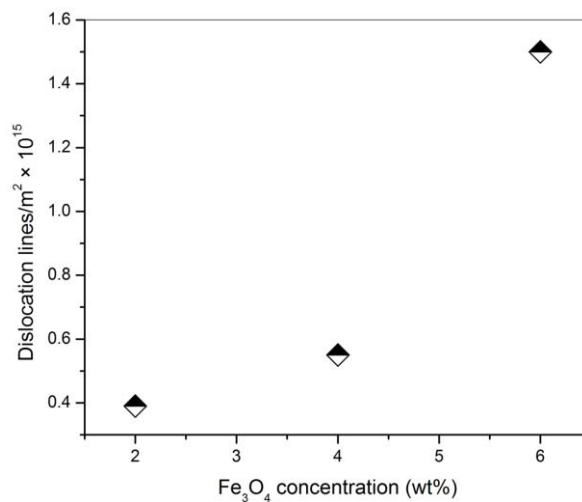


Fig. 3 Dislocation lines/m<sup>2</sup> (dislocation density) of doped zirconia NPs as a function of Fe<sub>3</sub>O<sub>4</sub> concentrations

As reported earlier (Denry and Kelly 2008) volume plays an important role for occurrence zirconia phase. Almost 3 to 5 % change in volume results in change in crystal structure volume of the unit cell of Fe<sub>3</sub>O<sub>4</sub> doped zirconia. Volume calculations show that shrinkage in volume with Fe<sub>3</sub>O<sub>4</sub> content. This shrinkage in volume usually results in tetragonal phase as depicted in XRD data [Fig. 1]. Density is another important factor for biological implants. Density of doped zirconia NPs increases with Fe<sub>3</sub>O<sub>4</sub> content.

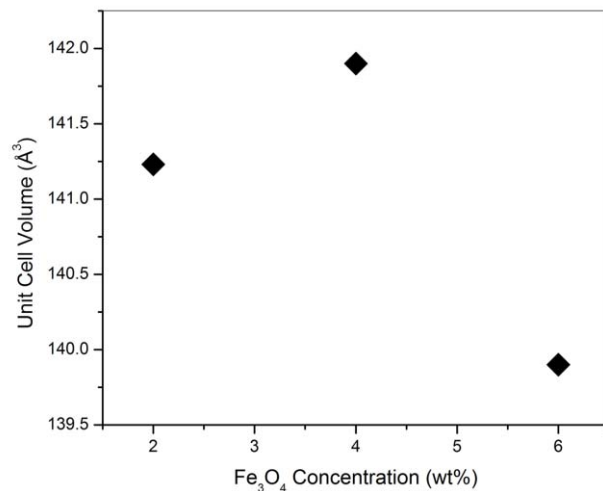


Fig. 4 Variation in unit cell volume with Fe<sub>3</sub>O<sub>4</sub> concentrations

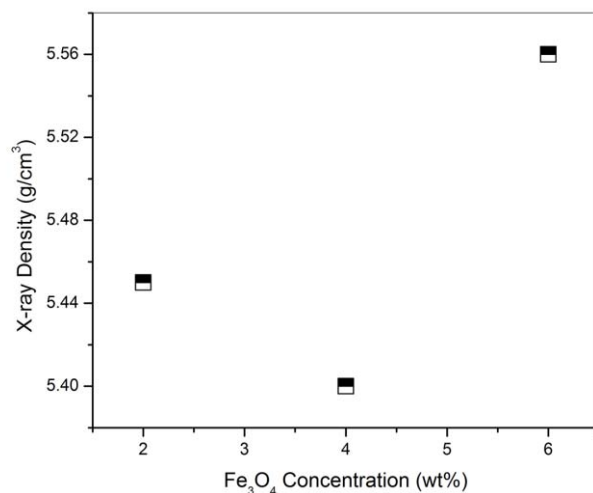


Fig. 5 Variation in X-ray density with Fe<sub>3</sub>O<sub>4</sub> concentrations

M-H curves for Fe<sub>3</sub>O<sub>4</sub> doped zirconia are shown in Fig. 6. Mixed behavior with paramagnetic and ferromagnetic has been observed in all the samples since curves do not saturate. This mixed behavior is due to mixing of two oxides having individual magnetic properties. Un-doped zirconia is paramagnetic in nature (Gionco et al. 2013) while doped NPs of Fe<sub>3</sub>O<sub>4</sub> are ferromagnetic (Riaz et al. 2014). Coercivity of Fe<sub>3</sub>O<sub>4</sub> doped zirconia NPs increases with Fe<sub>3</sub>O<sub>4</sub> content due to increase in amount of magnetic dopant as depicted in Fig. 7. However, low value of coercivity (~300Oe) is suitable for biological applications.

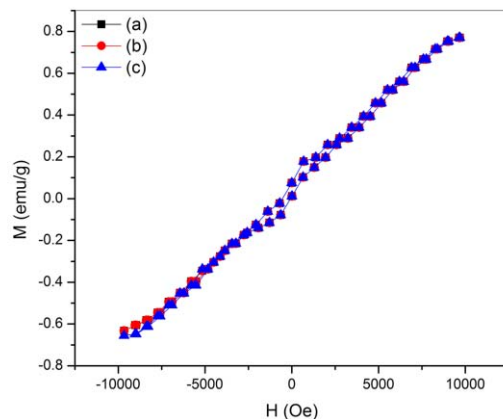


Fig. 6 M-H curves of Fe<sub>3</sub>O<sub>4</sub> doped zirconia NPs at (a) 2 (b) 4 and (c) 6wt%

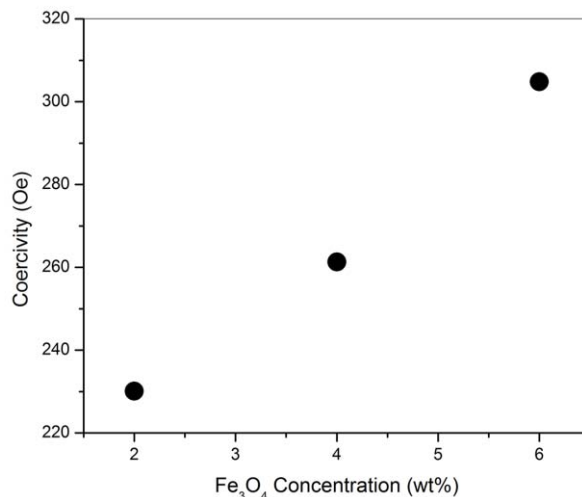


Fig. 7 Variation in coercivity with Fe<sub>3</sub>O<sub>4</sub> concentration

### 3. CONCLUSIONS

In this research articles Fe<sub>3</sub>O<sub>4</sub> doped zirconia NPs were prepared by using sol gel method. Fe<sub>3</sub>O<sub>4</sub> concentration was varied from 2 to 6wt%. XRD results revealed the formation of PSZ zirconia at room temperature. Crystallite size of samples decreased with the Fe<sub>3</sub>O<sub>4</sub> content due to substitution of smaller ionic radius atoms (Fe) with relatively larger ionic radius atoms (Zr). Shrinkage in volume and relatively higher density has observed at 6wt% of Fe<sub>3</sub>O<sub>4</sub> content. VSM results depicted the ferromagnetic behavior in doped samples with low value of coercivity. These synthesized NPs with high density and low value of coercivity can be successfully employed for biological implants as well as for cancer therapy.

## REFERENCES

- Balakrishnan, G., Thanigaiarul, K., Sudhakara, P., Song, J. (2013), "Microstructural and optical properties of nanocrystalline undoped zirconia thin films prepared by pulsed laser deposition", *Appl. Phys. A*, **110**, 427-432
- Bashir, M., Riaz, S. and Naseem, S. (2014a), "Fe<sub>3</sub>O<sub>4</sub> stabilized zirconia: structural, mechanical and optical properties", *J. Sol-Gel Sci. Technol.*, DOI: 10.1007/s10971-014-3415-4
- Bashir, M., Riaz, S. and Naseem, S. (2014b), "Fe<sub>3</sub>O<sub>4</sub> stabilized zirconia: structural, mechanical and optical properties", *IEEE Trans. Magn.*, DOI:10.1109/TMAG.2014.2312207
- Beg, S., Varshney, P., Sarita (2007), "Study of electrical conductivity changes and phase transitions in TiO<sub>2</sub> doped ZrO<sub>2</sub>", *J Mater Sci.*, **42**, 6274–6278.
- Davar, F., Hassankhani, A. and Estarki M.R.L. (2013), "Controllable synthesis of metastable tetragonal zirconia nanocrystals using citric acid assisted sol-gel method", *Ceram. Int.*, **39**, 2933–2941.
- Do-Nascimento, C., Issa, J.P.M., De-Oliveira, R.R., Iyomasa, M.M., Siéssere, S. and Regalo, S.C.H. (2007), "Biomaterials applied to the bone healing process", *Int. J. Morphol.*, **25**, 839-846.
- Fischer, D. and Kersch A. (2008), "The effect of dopants on the dielectric constant of HfO<sub>2</sub> and ZrO<sub>2</sub> from first principles," *Appl. Phys. Lett.*, **92**, 0129081-0129083\
- Gionco, C., Paganini, M.C., Giamello, E., Burgess, R., Valentin, C.D. and Pacchioni, G. (2013), "Paramagnetic Defects in Polycrystalline Zirconia: An EPR and DFT Study", *Chem. Mater.*, **25**, 2243–2253.
- Kazemi, F. (2011), "A Novel method for synthesis of metastable tetragonal zirconia nanopowders at low temperatures", *Ceram. Silikaty*, **55**, 26-30.
- Kohorst, P., Borchers, L., Stempel J., Stiesch, M., Hassel, T., Bach, F.W. and Hübsch C. (2012), *Acta Biomater.*, **8**, 1213-1220.
- Li, C., Li, K., Li, H., Zhang, Y., Ouyang, H., Liu, L. and Sun C. (2013), "Effect of reaction temperature on crystallization of nanocrystalline zirconia synthesized by microwave-hydrothermal process", *J. Alloy Compd.*, **561**, 23-27.
- Mueller, R., Jossen, R. and Pratsinis, S.E. (2004), "Zirconia Nanoparticles Made in Spray Flames at High Production Rates," *J. Am. Ceram. Soc.*, **87**,197–202.
- Nilsso, B., Korsgren, O., Lambris, J.D. and Ekdahl, K.N. (2010), "Can cells and biomaterials in therapeutic medicine be shielded from innate immune recognition?", *Trend Immunol.*, **31**, 32-38.
- Riaz, S., Bashir, M. and Naseem, S. (2014), "Iron oxide nanoparticles prepared by modified co-precipitation method," *IEEE Trans. Magn.*, **50**, 40033041-40033044.
- Riaz, S., Bashir, M., Hussain, S.S. and Naseem, S. (2013), "Effect of Mn doping Concentration on structural and magnetic properties of sol gel deposited ZnO diluted magnetic semiconductor", *Atlantis Press*, doi:10.2991/icacsei.2013.126
- Sahu, H.R. and Rao, G.R. (2000), "Characterization of combustion synthesized zirconia powder," *Bul. Mater. Sci.*, **23**, 349-354.
- Silva, R.F., DeOliveira, E.D., Filho, P.C.S. and Serra, C.R.N.A. (2011), "Diesel/biodiesel soot oxidation with CeO<sub>2</sub> and CeO<sub>2</sub>-ZrO<sub>2</sub>-modified cordierites: a facile way of

accounting for their catalytic ability in fuel combustion processes”, *Quim. Nova*, **34**, 759-763.

Somiya, S., Aldinger, F., Claussen, N., Spriggs, R.M., Uchino, K., Koumoto, K. and Kaneno, M. (2006), “Handbook of advance ceramics”, Academic Press United Kingdom.

Wei, G. and Ma, P.X. (2004), “Structure and properties of nano-hydroxyapatite/polymer composite scaffolds for bone tissue engineering”, *Biomater.*, **25**, 4749-4757.